PAPER

Preparation, structure and up-conversion luminescence properties of novel cryolite K_3YF_6:Er^{3+}, Yb^{3+}

Pengfei Shuai,[a] Dan Yang,[a] Libing Liao, [ID] *[a] Qingfeng Guo, [ID] *[bc] Lefu Mei,[a] Yidi Zhang[a] and Haikun Liu[a]

Cryolite is a suitable host for up-conversion luminescent materials due to its low phonon energy and good optical transparency. In this work, a novel up-conversion material K_3YF_6:Yb^{3+}, Er^{3+} with a cryolite structure was prepared successfully by a solid state method. The crystal structure, morphology, composition and up-conversion luminescence properties of the as-prepared sample were characterized by X-ray diffractometry (XRD), field emission scanning electron microscopy (SEM) and fluorescence spectrometer in detail. K_3YF_6:Er^{3+}, Yb^{3+} has a cryolite structure. Under 980 nm excitation, the as-prepared sample can generate slight green emission at 524 and 546 nm (attributed to $^2H_{11/2} \rightarrow {}^4I_{15/2}$ transition, $^4S_{3/2} \rightarrow {}^4I_{15/2}$ transition of Er^{3+}) and strong red emission at 661 and 672 nm (corresponding to $^4F_{9/2} \rightarrow {}^4I_{15/2}$ transition, $^4I_{9/2} \rightarrow {}^4I_{15/2}$ transition of Er^{3+}). All the green and red up-conversion emission of K_3YF_6:Er^{3+}, Yb^{3+} transfer and electronic transition process of the red and green light the sample emitted, the possible luminescence mechanism is discussed in this paper.

1. Introduction

Under the excitation of ultraviolet light, visible light or infrared light source, a material with certain luminescent properties is called photoluminescent material. Photoluminescent materials are classified into down-conversion luminescent materials and up-conversion luminescent materials, which are widely used in illumination sources, plasma displays, luminescent coatings, *etc.*[1–3] The material that absorbs short-wave radiation and then emits long-wave radiation is called a down-converting luminescent material, while the material that first absorbs long-wave radiation and then emits short-wave radiation is called an up-converting luminescent material. The up-converting luminescent material can be excited with low energy near infrared (NIR) radiation, and emits the light of higher energy in a visible range, due to the multi-photon absorption followed by an anti-Stokes emission.[4–8] So far, rare earth doped up-conversion materials have aroused widespread attention due to their important applications[9–14] in the fields of the national economy and national defense construction, such as in infrared quantum

counters, night vision systems, light-emitting diodes, other laser materials, *etc.*[15–18]

The urgent problem to be solved by up-converting luminescent materials is to find a suitable host. Although the host does not constitute an excitation level, it provides a suitable crystal field environment for the sensitizer ions and activator ions to cause matching energy level splitting to produce energy transfer and up-conversion luminescence.[19,20] At present, there are four main types of up-conversion host materials: oxide systems, sulfide-containing systems, halide systems (excluding fluorine), and fluoride systems. Compared to the other systems, the fluoride system has the advantages of low phonon energy, wide light transmission range, and easy to form waveguides and so on. Recently, fluoride has attracted the attention of researchers as the most popular up-conversion host.[21,22]

Cryolite, an important fluoride, has general formula of A_3BF_6 (A = Li, Na, K, NH_4, *etc.*; B = Al, Sc, V, Cr, Fe, Y, Ga, *etc.*), which is one of the most promising up-conversion host in the field of luminescent materials due to its low phonon energy, stable chemical composition and good optical transparency. Recently, compounds with cryolite structure have been widely used as host for luminescent materials, such as: K_3GaF_6:Mn^{4+},[23] Na_3GaF_6:Mn^{4+},[24] K_3LuF_6:Er^{3+},[25] K_3LuF_6:Ce^{3+}.[26] Na_3AlF_6:Mn^{4+} red phosphor was prepared *via* the coprecipitation and hydrothermal methods, and the phosphor was a promising candidate for application in warm WLEDs.[27] By controlling the concentration ratio of Eu^{3+}/Tb^{3+}, K_3LuF_6:Tb^{3+}, Eu^{3+} phosphors could be adjusted from green to yellowish pink.[28] K_3YF_6 is an a cryolite compound. Marek[29] reported the crystal structure and

[a]Beijing Key Laboratory of Materials Utilization of Nonmetallic Minerals and Solid Wastes, National Laboratory of Mineral Materials, School of Materials Sciences and Technology, China University of Geosciences, Beijing 100083, China. E-mail: clayl@cugb.edu.cn

[b]School of Gemology, China University of Geosciences, Beijing 100083, China. E-mail: qfguo@cugb.edu.cn

[c]Jewelry and Mineral Materials Laboratory of Experimental Teaching Demonstration Center, Beijing, China

vibrational properties of K_3YF_6 solid solution and considered it suitable as luminescent materials. These works mainly focus on the down-conversion of cryolite structure. So far, there is little research on K_3YF_6 to be used as an up-conversion host. In addition, Er^{3+}/Yb^{3+} doped monoclinic K_3YF_6 have not been reported.

Owing to the large absorption section and wide absorption region of Yb^{3+}, the up-conversion luminescence intensities of Er^{3+} are largely enhanced in (Er^{3+}, Yb^{3+}) co-doped materials. Some works of Er^{3+}/Yb^{3+} co-doped up-conversion luminescent material have been done, such as: $K_2GdF_5:Yb^{3+}/Er^{3+}$,[30] $Y_2O_3:Er^{3+}/Yb^{3+}$,[31] $Ba_2LaF_7:Er^{3+}/Yb^{3+}$,[32] $Na_5Lu_9F_{32}:Er^{3+}/Yb^{3+}$.[33]

Herein, a novel cryolite up-conversion luminescent material $K_3YF_6:Yb^{3+}$, Er^{3+} was successfully prepared by a solid state method. The crystal structure, elemental composition and up-conversion luminescence properties of the as-prepared samples were investigated in detail. Besides, the possible luminescence mechanism and electron transition process proposed were also discussed in this paper.

2. Experimental details

2.1 Synthesis

$K_3YF_6:Er^{3+}$, Yb^{3+} was prepared by a solid state method. The raw materials of K_2CO_3 (A.R.), NH_4HF_2 (A.R.), Y_2O_3 (99.99%), Er_2O_3 (99.99%) and Yb_2O_3 (99.99%) were purchased from Aladdin. The starting materials were weighted with electronic balance according to stoichiometric ratio. To prevent the fluorine from volatilizing during heating, NH_4HF_2 is treated with an excess of 30%. The weighed raw materials were ground in an agate mortar until well mixed. Then, they were transferred to a muffle furnace and calcined at 750 °C for 3 h. After cooling to room temperature, the samples were taken out and grinded into powder again for a series of test followed.

2.2 Measurement

The structure of the prepared samples was characterized by X-ray diffraction (XRD) measurements using an X-ray powder diffractometer (D8 Advance, Bruker, Germany; Cu Kα radiation, $\lambda = 0.15418$ nm) at 40 kV and 100 mA, and the step width is $0.02°$ (2θ) with 2θ ranging from 10 to $70°$. The morphology and energy dispersive X-ray (EDX) spectra of the as-prepared samples were obtained by a field emission scanning electron microscope (SEM, JSM-6701F, Hitachi, Japan) with 15 kV acceleration voltage. Under room temperature, the fluorescence emission spectra of samples were measured on a fluorescence spectrophotometer (Hitachi F4600) with an external tunable 980 nm infrared laser as excitation source.

3. Results and discussions

As we know, cryolite has two crystal forms, that is, mono-clinic and cubic. Fig. 1 shows the crystal structure for mono-clinic K_3YF_6 (space group $P2_1/n$). As shown in Fig. 1, Y^{3+} can occupy strongly distorted octahedral sites with centrosymmetric C_i local symmetry with six-fold coordinated by fluorine ions.[34]
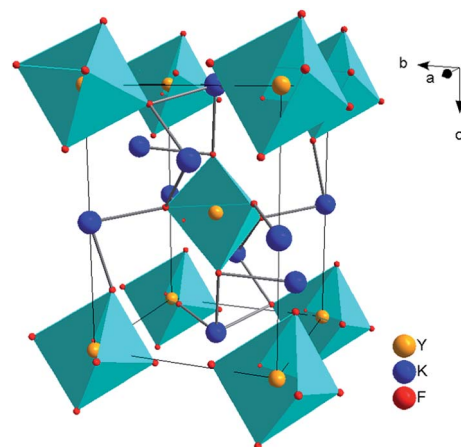

Fig. 1 Crystal structure of mono-clinic K_3YF_6.

Since the electricity valences and ionic radii of Yb^{3+}/Er^{3+} and Y^{3+} are close to each other, it is considered that Yb^{3+}/Er^{3+} replaces the site for Y^{3+} during the doping process.

The luminous efficiency of the up-converting luminescent material is not only related to the host structure, but also to the phase purity of the prepared material. Therefore, the structure of the prepared sample was analyzed by an X-ray powder diffractometer. Fig. 2 shows th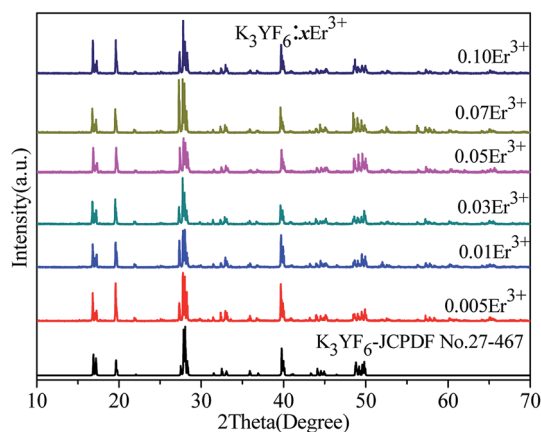e XRD patterns of $K_3YF_6:xEr^{3+}$ (x = 0.005, 0.01, 0.03, 0.05, 0.07, and 0.10), and the data for K_3YF_6 (JCPDF no. 27-467) is shown a reference. As illustrated in Fig. 2, the diffraction peak positions of the as-prepared samples match well with these of standard K_3YF_6 (JCPDF no. 27-467) without any impurity peak, indicating that all the as-prepared samples were cryolite compound. The increasing doping ratios of Er^{3+} did not cause K_3YF_6 structural changes.[35–37]

The emission spectra of as-prepared $K_3YF_6:xEr^{3+}$ (x = 0.005, 0.01, 0.03, 0.05, 0.07 and 0.10) samples are shown in Fig. 3. The centers of the six emission peaks are 526 ($^2H_{11/2} \rightarrow {}^4F_{15/2}$), 535 ($^2H_{11/2} \rightarrow {}^4F_{15/2}$), 548 ($^4S_{3/2} \rightarrow {}^4F_{15/2}$), 556 ($^4S_{3/2} \rightarrow {}^4F_{15/2}$), 661 ($^4F_{9/2} \rightarrow {}^4F_{15/2}$) and 672 nm ($^4I_{9/2} \rightarrow {}^4F_{15/2}$) in the green and red

Fig. 2 XRD patterns of $K_3YF_6:xEr^{3+}$ (x = 0.005, 0.01, 0.03, 0.05, 0.07, and 0.10), and the data for K_3YF_6 (JCPDF no. 27-467) is shown a reference.

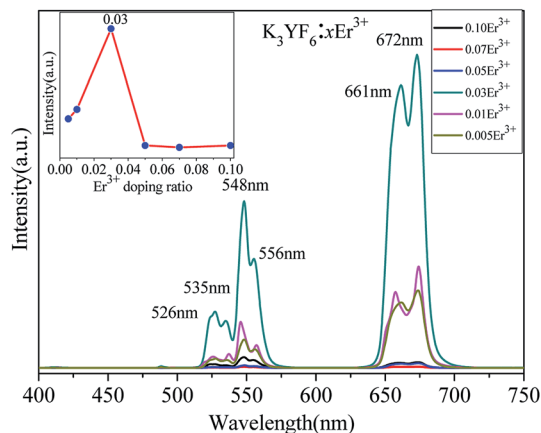Fig. 3 The emission spectra of K_3YF_6:xEr^{3+} (0.005, 0.01, 0.03, 0.05, 0.07 and 0.10) excited by 980 nm infrared laser, with the doping ratio dependences of emission intensity at 672 nm shown in the inset.

regions, respectively. Remarkably, for K_3YF_6:$0.03Er^{3+}$, the emission peak at 672 nm is the highest and the inset shows the dependence of luminescence intensity on the Er^{3+} doping ratio at 672 nm. With the increasing for Er^{3+} doping ratio from 0.005 to 0.10, the intensity of the emission peak of the samples firstly increased and then decreased and finally stabilized. When the Er^{3+} doping ratio was 0.03, the intensity of the emission peak at 672 nm was the highest. Fig. 4 shows the visual illumination of K_3YF_6:xEr^{3+} (x = 0.005, 0.01, 0.03, 0.05, 0.07, and 0.10) under 980 nm laser excite. As shown in Fig. 4, the emitted light changes from green to red, and the luminous intensity increases firstly and then decreases. When the Er^{3+} doping ratio

is 0.03, the sample is the brightest and present red. This lays the foundation for the preparation of the up-conversion luminescent material with excellent performance.

A series of Er^{3+}/Yb^{3+} co-doped K_3YF_6 up-conversion luminescent materials have been prepared. The microscopic, structures of the K_3YF_6:$0.03Er^{3+}$/yYb^{3+} (y = 0.01, 0.03, 0.07, 0.09, 0.12, 0.15, and 0.18) were determined. Fig. 5 shows the XRD patterns of K_3YF_6:$0.03Er^{3+}$/yYb^{3+} (y = 0.01, 0.03, 0.07, 0.09, 0.12, 0.15 and 0.18), and the data for K_3YF_6 (JCPDF no. 27-467) is shown a reference. It can be found that the diffraction peaks of the as-prepared samples match well with K_3YF_6 (JCPDS 27-467),
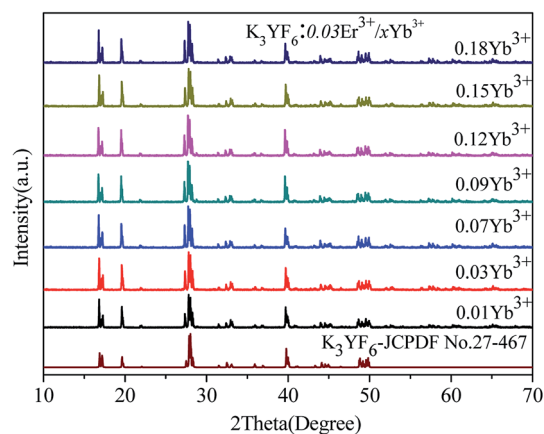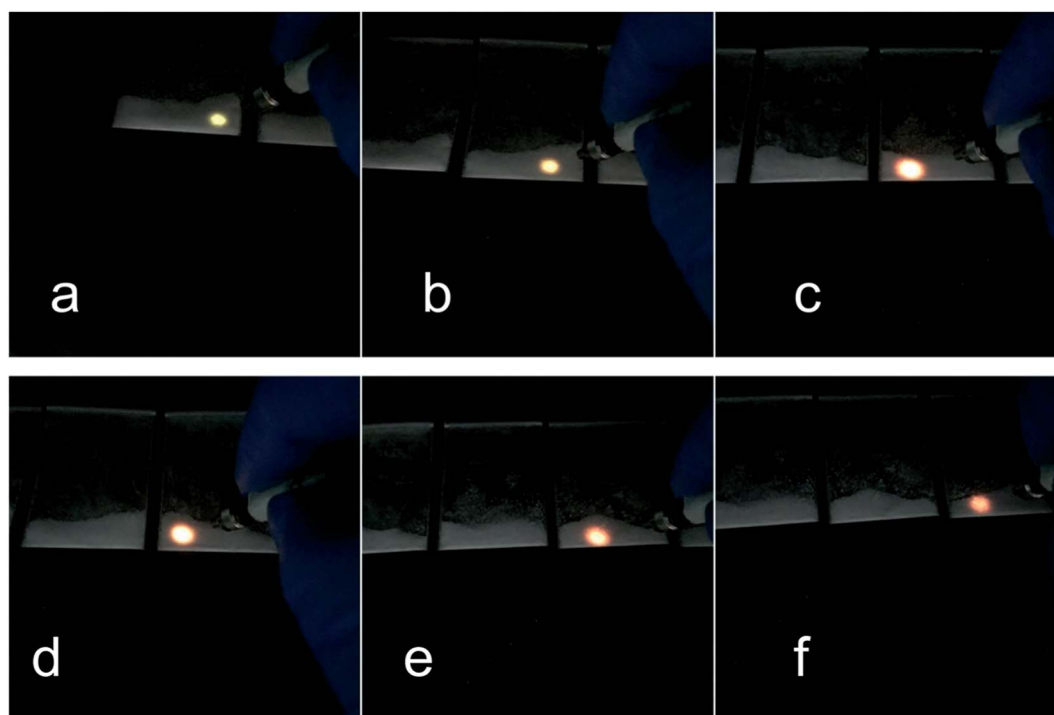

Fig. 5 XRD patterns of K_3YF_6:$0.03Er^{3+}$/yYb^{3+} (y = 0.01, 0.03, 0.07, 0.09, 0.12, 0.15 and 0.18), and the data for K_3YF_6 (JCPDF no. 27-467) is shown a reference.

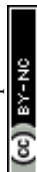Fig. 4 The luminescence of K_3YF_6:xEr^{3+} (x = 0.005 (a), 0.01 (b), 0.03 (c), 0.05 (d), 0.07 (e) and 0.10 (f)) under 980 nm laser irradiation.

indicating that Er^{3+}/Yb^{3+} co-doping does not change the crystal structure significantly.

Fig. 6 shows the SEM image and elemental mapping image of K_3YF_6:$0.03Er^{3+}$, $0.12Yb^{3+}$ sample (a) and the EDX spectrum of K_3YF_6:$0.03Er^{3+}$, $0.12Yb^{3+}$ (b). As shown in Fig. 6(a), the prepared sample appeared to be irregular particles with a grain size of about 10 μm. And the sample appear to partly agglomerate, which can be explained by the inhibition of grain growth due to the accumulation of vacancies on the grain boundaries when the Er^{3+}/Yb^{3+} with higher valency occupies the K^+ site. The element mapping results shown in Fig. 6(a) indicate that K, F, Y, Er, and Yb elements can be observed in K_3YF_6:$0.03Er^{3+}$, $0.12Yb^{3+}$, and all the elements in the sample are uniformly distributed. The K (31.5%), F (36.5%), Y (29.5%), Er (0.4%), and Yb (2.0%) peaks were observed in the EDX spectrum of Fig. 6(b), further indicating that the measured lanthanide atomic ratios of K_3YF_6:$0.03Er^{3+}$, $0.12Yb^{3+}$ are close to the calculated values.

The up-conversion emission spectra of K_3YF_6:$0.03Er^{3+}$, yYb^{3+} ($y = 0.01$, 0.03, 0.07, 0.09, 0.12, 0.15 and 0.18) are shown in Fig. 7. Four emission peaks at 524, 546, 661 and 672 nm in the green and red regions can be founded, which can be ascribed to the transitions from $^2H_{11/2}$, $^4S^{3/2}$, $^4F_{9/2}$, and $^4I_{9/2}$ states to $^4I_{15/2}$ state of Er^{3+}, respectively.[38,39] The inset shows the effect of Yb^{3+} doping ratio on the luminescence intensity of the K_3YF_6:$0.03Er^{3+}$, yYb^{3+} ($y = 0.01$, 0.03, 0.07, 0.09, 0.12, 0.15 and 0.18). With the increasing for Yb^{3+} from 0.01 to 0.18, the emission intensity of the samples firstly increased and then decreased. When the Yb^{3+} doping ratio was 0.12, the intensity of the emission peak at 672 nm was the highest. Fig. 8 is the visual illumination of K_3YF_6:$0.03Er^{3+}$, yYb^{3+} ($y = 0$, 0.01, 0.03, 0.07, 0.09, 0.12, 0.15 and 0.18) under 980 nm laser excite. As is shown in Fig. 8, the emitted light changes from light red to deep red, and the luminous intensity increases first and then decreases.
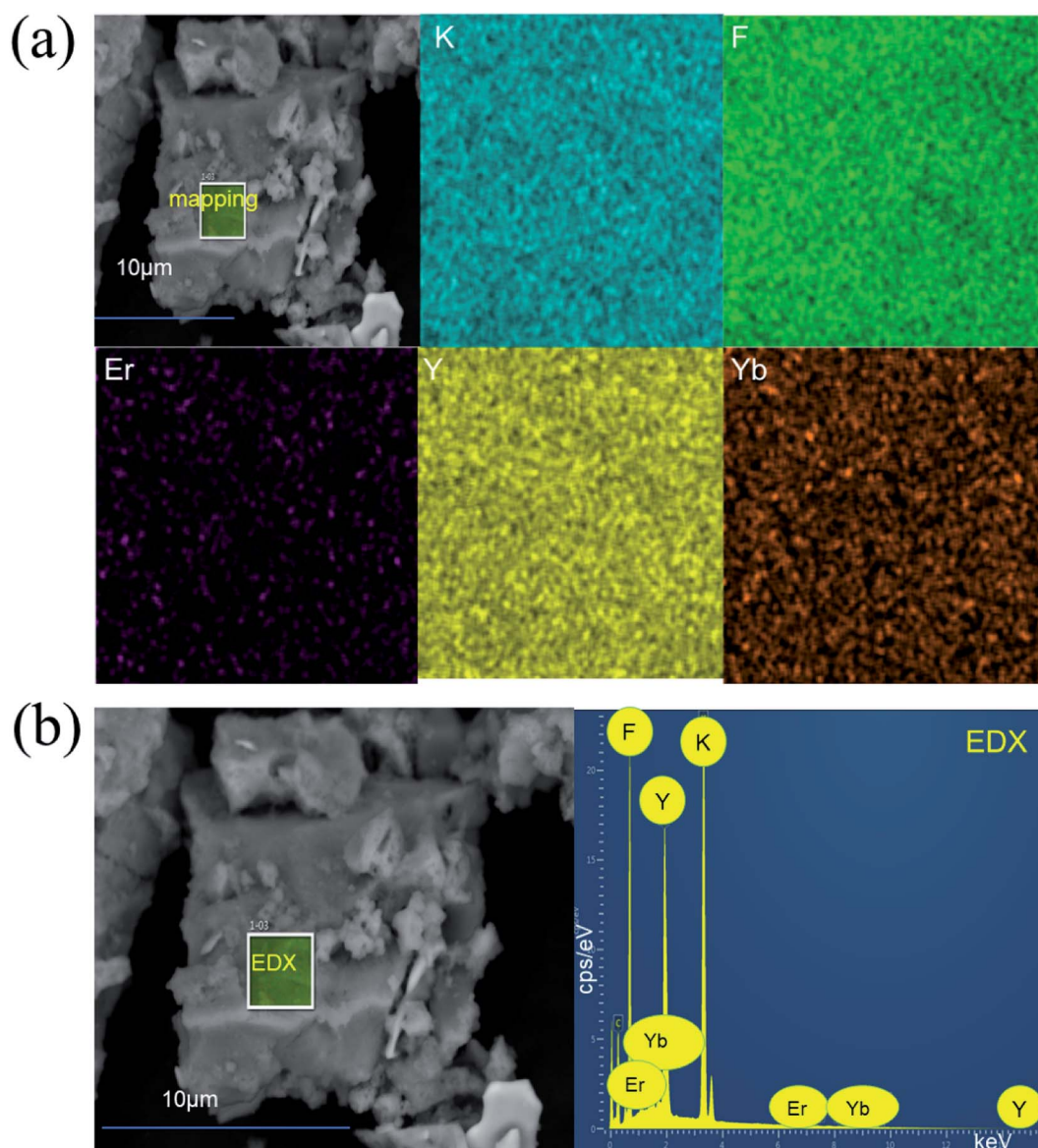

Fig. 6 (a) The SEM image and elemental mapping image of K_3YF_6:$0.03Er^{3+}$, $0.12Yb^{3+}$ sample; (b) the EDX spectrum of K_3YF_6:$0.03Er^{3+}$, $0.12Yb^{3+}$.
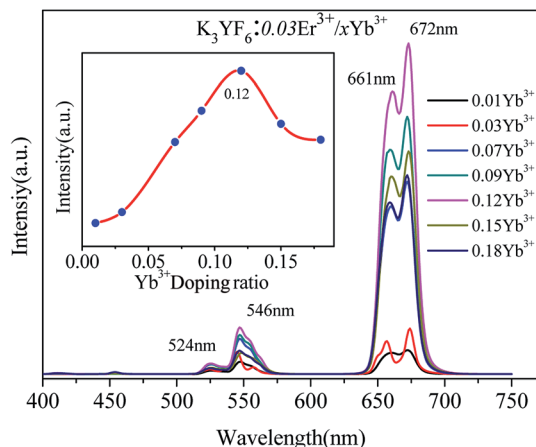
Fig. 7 Up-conversion emission spectrum of K_3YF_6:$0.03Er^{3+}$/yYb^{3+} (y = 0.01, 0.03, 0.07, 0.09, 0.12, 0.15 and 0.18) samples excited by 980 nm laser, with the doping ratio dependences of emission intensity at 672 nm shown in the inset.
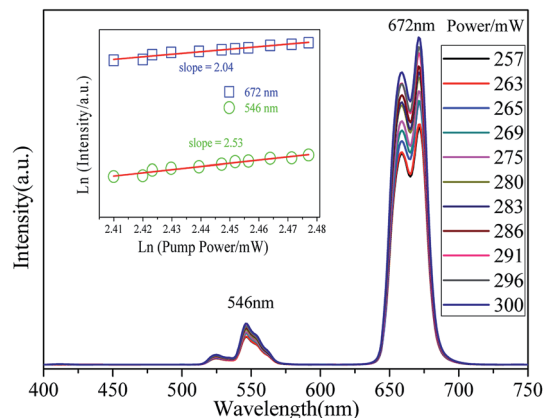

Fig. 9 Pump power dependence UC emission spectra of K_3YF_6:$0.03Er^{3+}$, $0.12Yb^{3+}$; and the inset shows lnarithmic plots of green and red UC emission intensity *versus* pump power for K_3YF_6:$0.03Er^{3+}$, $0.12Yb^{3+}$.

When the Yb^{3+} doping ratio is 0.12, the sample is the brightest and present deep red.

The pump power dependent UC emission spectra of K_3YF_6:$0.05Er^{3+}$, $0.12Yb^{3+}$ are shown in Fig. 9. With the increase of pump power from 257 to 300 mW, the up-conversion emission intensity shows an upward trend. The relationship between up-conversion intensity and excitation pump power can be applied as follow:

$$I \propto P^n$$

In which I and P are the intensity of the up-conversion emission and the power of the excitation pump, respectively. n represents

the number of phonons that need to populate the upper excited state energy level.[30] In order to obtain the value of n, the double logarithmic figure of the emission intensity of green and red up-conversion emission with pump power for K_3YF_6:$0.05Er^{3+}$, $0.15Yb^{3+}$ were depicted in inset of Fig. 9 The green and red dots represent up-conversion emission peaks at 546 and 672 nm, respectively. The experimental data are fitted in a straight line. The n values of green and red up-conversion lines are calculated to be 2.53 and 2.04, respectively. The number of n is near to 2, indicating that the green and red up-conversion emission of K_3YF_6:$0.03Er^{3+}$, $0.12Yb^{3+}$ all belong to two-photon process.[40]

The possible up-conversion luminescence mechanism and electron transition process for the sample of K_3YF_6:$0.01Er^{3+}$, $0.12Yb^{3+}$ to emit red and green light are shown in Fig. 10. Under
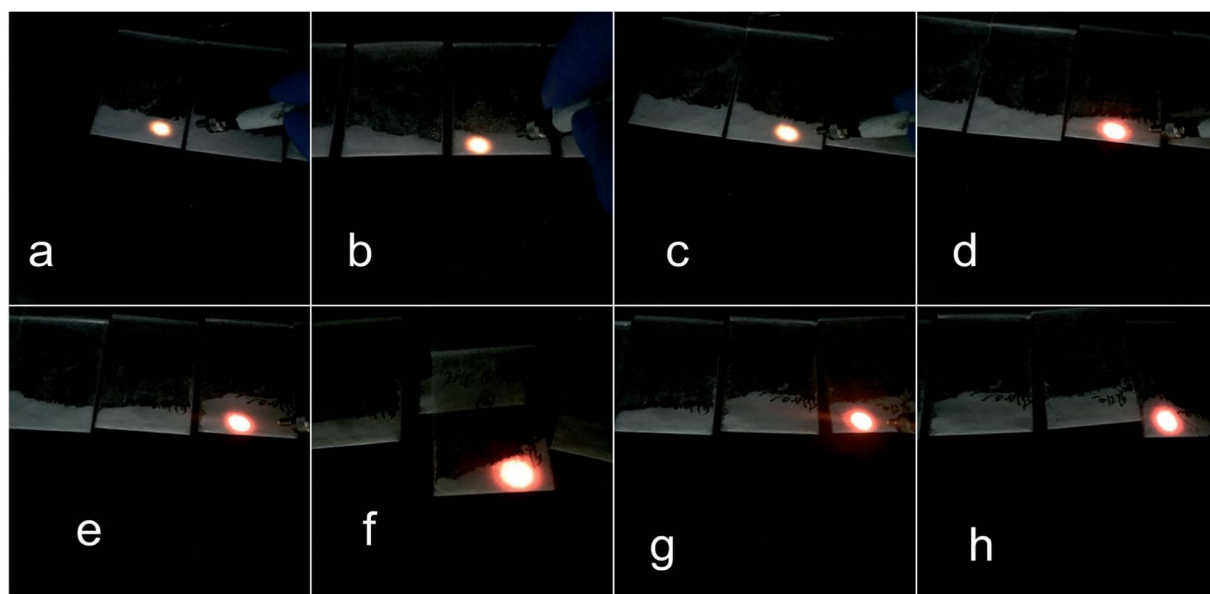

Fig. 8 The luminescence of K_3YF_6:$0.03Er^{3+}$, yYb^{3+} (y = 0 (a), 0.01 (b), 0.03 (c), 0.07 (d), 0.09 (e), 0.12 (f), 0.15 (g) and 0.18 (h)) under 980 nm laser irradiation.
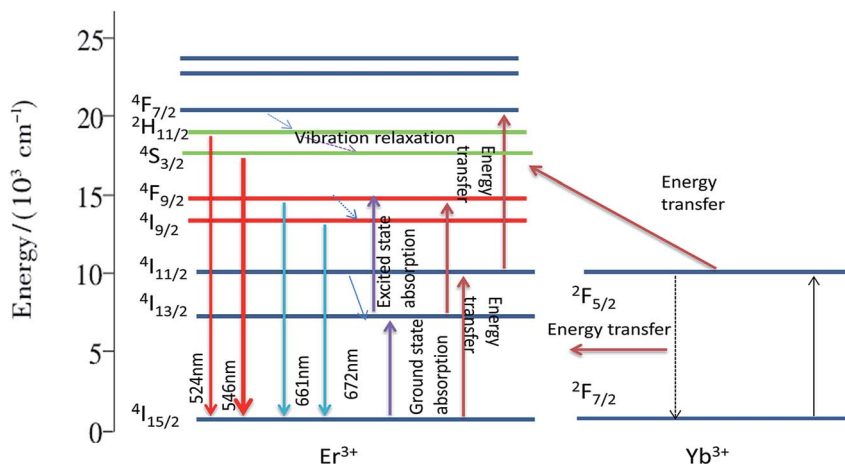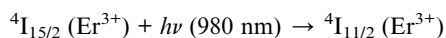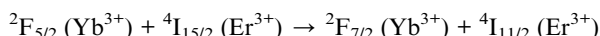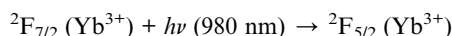
Fig. 10 K_3YF_6:0.03Er^{3+}, 0.12Yb^{3+} up-conversion luminescence mechanism.

980 nm laser excitation, the electron of the sensitizer Yb^{3+} absorbs a 980 nm photon from the energy level $^2F_{7/2}$ to the $^2F_{5/2}$ level. When the excited state is unstable, the electrons of Yb^{3+} will return to the $^2F_{7/2}$ level through the non-radiative transition, and the energy released during the transition will be transferred to the activator Er^{3+}. The electrons in the ground state of Er^{3+} absorb the energy transmitted by Yb^{3+} and transited to the $^4I_{11/2}$ level. Since the Er^{3+} and Yb^{3+} levels match very well, the electrons of the activator Er^{3+} can also directly absorb a photon of 980 nm from the ground state level $^4I_{15/2}$ to the $^4I_{11/2}$ excited state level. The specific process is as follows:

$$^2F_{7/2} (Yb^{3+}) + h\nu (980 \text{ nm}) \rightarrow {}^2F_{5/2} (Yb^{3+})$$

$$^2F_{5/2} (Yb^{3+}) + {}^4I_{15/2} (Er^{3+}) \rightarrow {}^2F_{7/2} (Yb^{3+}) + {}^4I_{11/2} (Er^{3+})$$

$$^4I_{15/2} (Er^{3+}) + h\nu (980 \text{ nm}) \rightarrow {}^4I_{11/2} (Er^{3+})$$

Some electrons at the $^4I_{11/2}$ level of Er^{3+} directly accept the energy released from the electronic transition in the excited state of Yb^{3+} back to the ground state, and jump up to the $^4F_{7/2}$ level. Since the energy gap between $^4F_{7/2}$ and $^2H_{11/2}$, $^2H_{11/2}$ and $^4S_{3/2}$ is small, electrons at the $^4F_{7/2}$ level will quickly relax to the $^2H_{11/2}$/$^4S_{3/2}$ level without radiation. When the electron absorption energy at the $^4I_{13/2}$ level shifts to the $^4F_{9/2}$ level, the electrons of the $^4F_{9/2}$ level will undergo a non-radiative transition to $^4I_{9/2}$, and the electron will go back to the ground state of the $^4I_{9/2}$ and $^4F_{9/2}$ levels.

4. Conclusions

A series of up-conversion luminescent materials K_3YF_6:Er^{3+}, Yb^{3+} with cryolite structure were prepared by a solid state method for the first time. XRD results indicated that all prepared K_3YF_6:Er^{3+}, Yb^{3+} samples were pure phase, belonging to monoclinic system, space group $P2_1/n$. Under the 980 nm light exhibition, the K_3YF_6:Er^{3+}, Yb^{3+} shows typical transition of Er^{3+}, which composed of two parts in the visible region that green and red. When the doping ratio of $Er^{3+}$is 0.03 and the

doping ratio of $Yb^{3+}$is 0.12, the luminous intensity reaches the maximum. According to the relation between the up-conversion intensity and the excitation pump power at 980 nm laser excitation, the two-photon process dominated in the red and green up-conversion processes of Er^{3+} ions. All the results indicated K_3YF_6:0.03Er^{3+}, 0.12Yb^{3+} is an excellent up-conversion luminescent material.

Conflicts of interest

There are no conflicts to declare.

Acknowledgements

References

1 J. Y. Sun, H. Y. Du and W. X. Hu, *Solid luminescent materials*, Chemical Industry Press, 2003.
2 J. Y. Li, *Rare earth luminescent materials and their applications*, Chemical Industry Press, 2003.
3 Y. Y. Liu and X. Wang, Controllable synthesis and up-conversion luminescence properties of Yb^{3+}/Er^{3+} codoped $(MLaFn)_x$ ($M = 0$, K; $n = 3$, 4; $x = 1$, 1.5) of nanomaterials, *Chin. J. Lumin.*, 2019, **40**(2), 1000–7032.
4 G. Y. Zhang, Q. P. Qiang, S. S. Du and Y. H. Wang, An up-conversion luminescence and temperature sensor based on Yb^{3+}/Er^{3+}co-doped $GdSr_2AlO_5$, *RSC Adv.*, 2018, **8**, 9512–9518.
5 N. Z. Zhang, M. S. Molokeev, Q. L. Liu and Z. G. Xia, Pure red up-conversion luminescence and optical thermometry of Er^{3+} doped sensitizer-rich $SrYbInO_4$ phosphors, *J. Mater. Chem. C*, 2018, **6**, 7361–7366.
6 W. Xu, X. Chen and H. W. Song, Manipulation of local electromagnetic field in up-conversion luminescence of rare earth ions, *Chin. J. Lumin.*, 2018, **39**(1), 1–26.

7 Y. Fu, J. Leng, M. M. Xing, Y. Tian and X. X. Luo, Synthesis and luminescence properties of Ca$_3$Y$_2$Si$_3$O$_{12}$:Tm^{3+}, Yb^{3+} up-conversion phosphors, *Chin. J. Lumin.*, 2017, **38**(5), 561–566.

8 X. W. Yao, G. F. Yao, Y. Li and J. S. Zhang, Synthesis and up-conversion luminescence of NaLuF$_4$: Yb^{3+}, Er^{3+} microcrystals, *Chin. J. Lumin.*, 2013, **34**(10), 1319–1323.

9 Y. M. Yang, F. Y. Jiao, H. X. Su and Z. Q. Li, Preparation and up-conversion efficiencies of Yb^{3+}, Er^{3+} co-doped BaGd$_2$ZnO$_5$, *Chin. J. Lumin.*, 2012, **33**(12), 1319–1323.

10 L. Zhao, D. Meng, Y. Li, Y. Zhang and H. Wang, Tunable emitting phosphors K$_3$Gd(PO$_4$)$_2$:Tm^{3+}/Dy^{3+} for light-emitting diodes and field emission displays, *J. Alloys Compd.*, 2017, **728**, 564–570.

11 I. E. Kolesnikov, A. A. Kalinichev, M. A. Kurochkin, D. V. Mamonova, E. Yu. Kolesnikov and E. Lähderanta, Ratiometric optical thermometry based on emission and excitation spectra of YVO$_4$:Eu^{3+} nanophosphors, *J. Phys. Chem. C*, 2019, **123**, 5136–5143.

12 J. K. Zaręba, M. Nyk, J. Janczak and M. Samoć, Three-photon absorption of coordination polymer transforms UV-to-VIS thermometry into NIR-to-VIS thermometry, *ACS Appl. Mater. Interfaces*, 2019, **11**, 10435–10441.

13 Z. L. Wu, H. M. Wu and Z. Yao, Up-conversion luminescence and temperature characteristics of GdNbO$_4$:Er^{3+}/Yb^{3+} Phosphors, *Chin. J. Lumin.*, 2017, **38**(9), 1129–1135.

14 G. F. Liu and Z. L. Fu, Synthesis and temperature sensing of CaF$_2$:Er^{3+}, Yb^{3+} nanoparticles with up-conversion fluorescence, *Chin. J. Lumin.*, 2017, **38**(2), 133–138.

15 G. Tripathi, V. K. Rai and S. B. Rai, Up-conversion and temperature sensing behavior of Er^{3+}, doped Bi$_2$O$_3$–Li$_2$O–BaO–PbO tertiary glass, *Opt. Mater.*, 2007, **30**(2), 201–206.

16 X. Wang, M. Lan, Y. Z. Yang, L. L. Wang, Z. H. Sun and W. W. Wang, Synthesis and enhanced up-conversion optical properties of Cu^{2+} Ion doped β-NaYF$_4$:Yb^{3+}, Er^{3+} crystals, *Chin. J. Lumin.*, 2018, **39**(8), 1082–1086.

17 J. Wang, R. Deng, M. A. MacDonald, B. Chen, J. Yuan, F. Wang, D. Chi, T. S. Hor, P. Zhang, G. Liu, Y. Han and X. Liu, Enhancing multiphoton up-conversion through energy clustering at sublattice level, *Nat. Mater.*, 2014, **13**, 157–162.

18 W. Zou, C. Visser, J. A. Maduro, M. S. Pshenichnikov and J. C. Hummelen, Broadband dye-sensitized up-conversion of near-infrared light, *Nat. Photonics*, 2012, **6**, 560–564.

19 H. Li and L. Wang, NaYF$_4$:Yb^{3+}/Er^{3+} nanoparticle-based up-conversion luminescence resonance energy transfer sensor for mercury (II) quantification, *Analyst*, 2013, **138**(5), 1589–1595.

20 J. Zhang, C. Mi and H. Wu, Synthesis of NaYF$_4$:Yb/Er/Gd up-conversion luminescent nanoparticles and luminescence resonance energy transfer-based protein detection, *Anal. Biochem.*, 2012, **421**(2), 673–679.

21 Y. Yu, D. Qi and H. Zhao, Enhanced green up-conversion luminescence in Ho^{3+}/Yb^{3+} codoped Y$_2$O$_3$, ceramics with Gd^{3+}, *J. Lumin.*, 2013, **143**(6), 388–392.

22 P. Bhoyar and S. J. Dhoble, Electron-vibrational interaction in 5d state of Eu^{2+} in LiMgBF$_6$, Li$_2$NaBF$_6$, and Li$_3$BF$_6$:Eu^{2+} phosphors, *J. Lumin.*, 2013, **139**, 22–27.

23 T. T. Deng, E. H. Song and Y. Y. Zhou, Stable narrowband red phosphor K$_3$GaF$_6$:Mn^{4+} derived from hydrous K$_2$GaF$_5$ (H$_2$O) and K$_2$MnF$_6$, *J. Mater. Chem. C*, 2017, **5**, 9588–9596.

24 T. T. Deng, E. H. Song, J. Sun, L. Y. Wang, Y. Deng, S. Ye, J. Wang and Q. Y. Zhang, Design and preparation of thermally stable Mn^{4+} ions activated narrowband red emitting fluoride Na$_3$GaF$_6$:Mn^{4+} for warm WLED application, *J. Mater. Chem. C*, 2017, **11**, 2910–2918.

25 J. k. Cao, Research on temperature sensing characteristics based on K$_3$LuF$_6$:Er^{3+} glass-ceramic glass green up-conversion, *J. Chin. Rare Earth Soc.*, 2017, 124.

26 D. Yang and H. k. Liu, Crystal structure and luminescence properties of a novel cryolite-type K$_3$LuF$_6$:Ce^{3+} phosphor, *J. Solid State Chem.*, 2019, **277**, 32–36.

27 F. Hong, H. P. Xu, G. X. Liu and C. Song, Mn^{4+} nonequivalent-doped Al^{3+}-based cryolite high-performance warm WLED red phosphors, *New J. Chem.*, 2019, **43**, 14859–14871.

28 D. Yang, L. B. Liao and Q. F. Guo, Luminescence properties and energy transfer of K$_3$LuF$_6$:Tb^{3+}, Eu^{3+} multicolor phosphors with a cryolite structure, *RSC Adv.*, 2019, **9**, 4295–4302.

29 A. G. Marek, G. Anna, T. G. Monika and R. R. Witold, Crystal structure and vibrational properties of new luminescent hosts K$_3$YF$_6$ and K$_3$GdF$_6$, *J. Solid State Chem.*, 2006, **179**, 3145–3150.

30 F. F. Chi, F. F. Hu, X. T. Wei, Y. H. Chen and M. Yi, Synthesis and thermometric properties of Yb^{3+}/Er^{3+} co-doped K$_2$GdF$_5$ up-conversion phosphors, *J. Rare Earths*, 2017, **35**(5), 436–440.

31 C. Joshi, A. Dwivedi and S. B. Rai, Structural morphology, up-conversion luminescence and optical thermometric sensing behavior of Y$_2$O$_3$:Er^{3+}/Yb^{3+} nano-crystalline phosphor, *Spectrochim. Acta, Part A*, 2014, (129), 451–456.

32 J. M. Hu, D. C. Zhou and J. B. Qiu, Up-conversion of Er^{3+}/Yb^{3+} co-doped transparent glass-ceramics containing Ba$_2$LaF$_7$ nanocrystals, *J. Rare Earths*, 2013, **31**(9), 843–848.

33 X. Zhou, H. Wang and B. J. Chen, Efficient up-conversion Yb^{3+}, Er^{3+}co-doped Na$_5$Lu$_9$F$_{32}$ single crystal for photovoltaic application under solar cell spectrum excitation [J], *Chin. Opt. Lett.*, 2019, **17**(09), 72–76.

34 M. A. Gusowski, A. Gagor, M. Trzebiatowska-Gusowska and W. Ryba-Romanowski, Crystal structure and vibrational properties of new luminescent hosts K$_3$YF$_6$ and K$_3$GdF$_6$, *J. Solid State Chem.*, 2006, **179**, 3145–3150.

35 M. Runowski, S. Goderski, J. Paczesny, M. Księżopolska-Gocalska, A. Ekner-Grzyb, T. Grzyb, J. D. Rybka, M. Giersig and S. Lis, Preparation of biocompatible, luminescent-plasmonic core/shell nanomaterials based on lanthanide and gold nanoparticles exhibiting SERS effects, *J. Phys. Chem. C*, 2016, **120**(41), 23788–23798.

36 B. Li, X. Huang and J. Lin, Single-phased white-emitting Ca$_3$Y(GaO)$_3$(BO$_3$)$_4$:Ce^{3+}, Tb^{3+}, Sm^{3+} phosphors with high-efficiency: Photoluminescence, energy transfer and application in near-UV-pumped white LEDs, *J. Lumin.*, 2018, **204**, 410–418.

37 S. Q. Liu, Y. J. Liang, Y. L. Zhu, H. R. Li, Y. X. Cai and D. Tu, Full visible spectra emission introduced by crystal-site engineering in β-Ca₃(PO₄)₂-type solid solution phosphors for high quality white light emitting diodes application, *Chem. Eng. J.*, 2019, 375.

38 P. Liu, F. Wang, X. Chen and B. Yang, Up-conversion/Down-conversion luminescence and preparation of NIR-to-UV-excited Gd₂O₂S:Er phosphor, *J. Lumin.*, 2018, **200**, 126–132.

39 M. Hirano and K. Ishikawa, Hydrothermal formation and up-conversion luminescence of Er³⁺ doped GdNbO₄, *J. Am. Ceram. Soc.*, 2017, **100**, 2814–2821.

40 Y. L. Wei, X. M. Li and H. Guo, Enhanced up-conversion in novel KLu₂F₇:Er³⁺ transparent oxyfluoride glass-ceramics, *Opt. Mater. Express*, 2014, **4**, 1367–1372.